Physiotherapeutic treatment and clinical evaluation of shoulder disorders

Vermeulen, H.M.

5 3D SHOULDER POSITION MEASUREMENTS USING A SIX-DEGREE-OF-FREEDOM ELECTROMAGNETIC TRACKING DEVICE

C.G.M. Meskers[1] H.M. Vermeulen[2], J.H. de Groot[3], F.C.T. van der Helm[3], P.M. Rozing[1]
[1]Orthopaedic Laboratory, Dept. of Orthopaedics, Leiden University Medical Center
[2]Dept. of Physical Therapy, Leiden University Medical Center
[3]Man Machine Systems and Control Group, Laboratory for Measurement and Control, Dept. of Mechanical Engineering and Marine Technology, Delft University of Technology

Clinical Biomechanics 13 (1998) 280–292

Abstract

Objective: To describe a recording and processing methodology for obtaining kinematic data of the shoulder which meets three more criteria besides usual requirements regarding precision and accuracy: sufficient speed, obtaining complete 3D kinematics including joint rotations, and usage of coordinate systems based on reference points.

Design: Static recordings of shoulder bone orientations during standardized humerus elevations based on the palpation technique using a six-degree-of-freedom electromagnetic tracking device.

Background: An easy, fast, well standardized measurement methodology for obtaining complete 3D shoulder kinematic data is urgently needed for fundamental musculoskeletal and clinical research.

Methods: A measurement methodology was designed and developed. Shoulder kinematics were obtained from repeated measurements on 15 healthy subjects performed by two observers. Inter-trial, inter-day, inter-observer and inter-subject variability were established. Results were compared to literature.

Results: Complete kinematic descriptions were obtained. A measurement speed of about one position per second could be reached. The measured kinematics and accuracy of the measurements were found to be in concordance with the literature.

Conclusion: All previously formulated criteria for a clinical useful method for obtaining shoulder kinematics have been met.

Relevance: Obtaining 3D descriptions of shoulder motions of patients suffering from various pathologies as the impingement syndrome, glenohumeral (sub) luxation, adhesive capsulitis and shoulder function after arthroplasty is of vital importance in the search for etiology and pathogenesis of these disorders and for clinical evaluation.

Introduction

Because of the fact that a number of shoulder disorders show a malpositioned scapula (e.g., winging scapula in recurrent luxation of the shoulder or a disturbed scapulo humeral rhythm in patients with frozen shoulder) the explanation of this phenomenon and the definition of its relation to the course of the disease may be a key factor in fundamental understanding of etiology and pathogenesis of shoulder disorders. For clinical evaluation of shoulder pathology a useful methodology for measuring three-dimensional (3D) shoulder positions is therefore urgently needed. Furthermore, 3D positions of shoulder bones are the input for 3D inverse quasi-static shoulder modeling that allows for analysis of e.g., muscle forces and joint reaction forces. [1,2] The combination of a 3D kinematic measurement method with a shoulder model is a very powerful tool in clinical research. It will, for example, allow for biomechanical analysis of a clinical problem like loosening of the glenoid component in total shoulder arthroplasty [3], but one can think of many other applications.

Shoulder measurements should be in 3D and should be of sufficient precision and accuracy. In addition, a clinical useful method should meet three more criteria. First, a full description of the shoulder kinematics should be obtained, i.e., rotations of all four bony structures of the shoulder kinematic chain, namely, thorax, clavicle, scapula and humerus together with the interrelations between the bones: the rotations at the scapula-thoracic, sterno-clavicular, acromio-clavicular and glenohumeral joint. The underlying reason is that 3D shoulder modeling requires full kinematic input. [1,2] Furthermore, a complete kinematic description allows for the assessment of important clinical parameters as rotations at especially the glenohumeral joint. [4–6] Second, the measurements should be standardized to allow for comparisons of results. Standardization implicates both parametrization of the kinematics according to a well-defined protocol[6] and description of the motions of the local coordinate systems with respect to reference coordinate systems. [4–6] Third, the method should allow for fast and easy to perform measurements, so it becomes possible to measure larger groups of patients. This is of vital importance for building up extensive databases in which biomechanical as well as clinical parameters are stored, analogous to the CAMARC project regarding gait disorders.[7]

To our knowledge, there is no method described yet that meets all our criteria. Van der Helm and Pronk[5] developed a methodology based on the palpation technique that allowed for a full description of 3D shoulder kinematics which where well standardized. According to this methodology, the 3D positions of bony landmarks of the shoulder were obtained using a spatial linkage digitizer. [8] On the bony landmarks, local coordinate systems were constructed. In this way, the coordinate systems were based upon standard (anatomical) reference points. Rotations were parametrized to Cardan angles according to a fixed protocol defining initial positions, coordinate systems and decomposition orders. However, the use of a spatial linkage digitizer implied time consuming measurements, for every bony landmark had to be measured separately. Johnson et al[9] solved this problem by mounting the sensor of a six-degree- of-freedom electromagnetic tracking device on a 'scapula locator': a triangular device, which had to be adjusted manually over the scapula. In this way, the scapula rotations could be

obtained in one instant. The work by Johnson et al however did not include measurements of the total shoulder kinematic chain, i.e., thorax, clavicle, scapula and humerus. Furthermore, they were not able to link the measurements to reference coordinate systems. In order to overcome the disadvantages of each method it seems an obvious choice to combine the advantages of both methods. We therefore developed a palpation based method using a six-degree-of-freedom electromagnetic tracking device in combination with a scapula locator and a stylus. A stylus is a receiver mounted on a pointer, which can be used to digitize bony landmarks in the local coordinate systems of the receiver placed on the subject's shoulder.

The aim of this paper is to describe the complete shoulder kinematic data recording and processing methodology developed. Furthermore, a validation of the methodology will be presented, based on intra-subject and inter-observer repeated measurements on ten healthy subjects. Results from these measurements are compared with results from a previous study by Van der Helm and Pronk, processed by a similar data processing protocol but using data collected by means of a spatial linkage digitizer. A brief discussion of the measurement accuracy will be presented. Finally, the methodology will be evaluated in the light of using the measurement method as a clinical tool.

Methods

Measurement device

A six-degree-of-freedom electromagnetic tracking device 'Flock of Birds' (Ascension Technology, Burlington, VT) was used. This system consists of a transmitter and several receivers. The position vector ${}^{G}\mathbf{o}$ of the receivers with respect to the transmitter's center is recorded as well as the orientation of the receiver, here described as rotations around the global (= transmitter) x, y and z axes. We used an extended range transmitter with a measurement range of 0.45–2.4 m. All settings were in the default mode. A position calibration procedure was performed prior to the measurements, since the disturbance of metal in the environment, e.g., iron-strengthened concrete, is quite large. The mean residual errors after calibration were 2.07 mm for the x-coordinate, 2.38 mm for the y-coordinate and 2.35 mm for the z-coordinate.

Receivers

Three receivers were used to measure the rotations of the thorax, scapula and humerus. Using double-sided tape and Fixomull stretch self-adhesive bandage (Beiersdorf AG, Hamburg) the thorax receiver was glued to the sternum, somewhere between the incisura jugularis (IJ) and the processus xiphoideus (PX). The humerus receiver was mounted on a circular cuff, which could be adjusted tightly around the upper arm. The scapula receiver was mounted on a three-pin device according to Johnson et al [9]. This device was constructed as follows: two beams made of plexiglas are connected in

the middle like a cross. Three rods, moving in slots on either side of the beams, were positioned on the angulus acromialis (AA), the trigonum spinae (TS) and the angulus inferior (AI) (Figure 5.1). Once the locator is fitted over an individual scapula, the rods can be fixed so that a stiff construction is obtained. A fourth receiver was mounted on a pointed stylus of about 65 mm length.

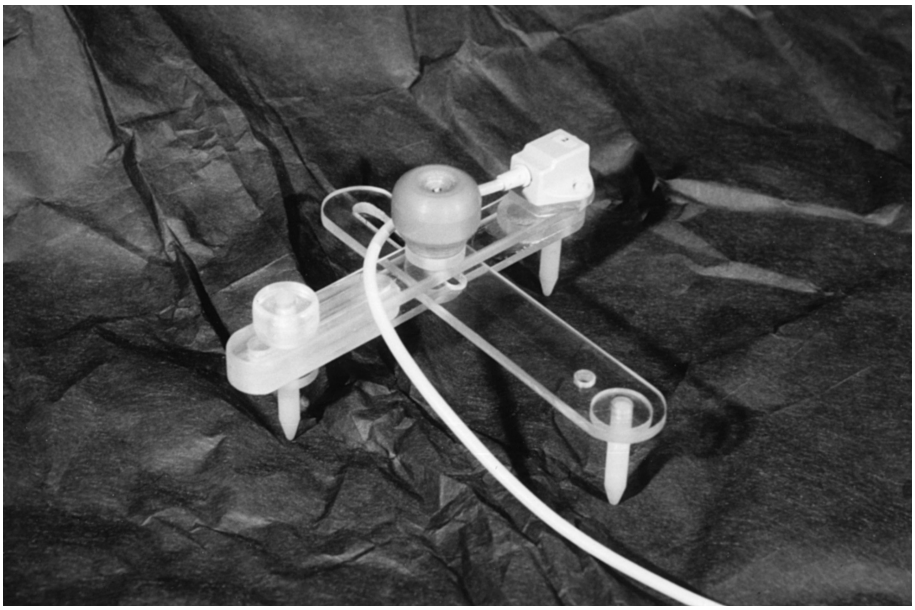

Figure 5.1. The scapula locator. The right upper rod is to be placed on AA, the left upper one on TS and the caudal one on AI. On the right upper side the receiver is mounted.

Initial measurements

In order to be able to reconstruct the 3D positions of the bony landmarks of the shoul - der bones, initial measurements were performed. With the subject in a resting position with the arms hanging aside the body, 12 bony landmarks were palpated and subse - quently touched with the stylus endpoint (Table 5.1). The position and orientation of the stylus receiver were then recorded together with the position and orientation of the receivers mounted on the thorax and the humerus (hereafter called the bone receivers). The 3D coordinates of the stylus endpoint in the global coordinate system were calcu - lated by:

$$\begin{bmatrix} s_x \\ s_y \\ s_z \end{bmatrix} = \begin{bmatrix} o_{sx} \\ o_{sy} \\ o_{sz} \end{bmatrix} + (R_x(\alpha_s) \cdot R_y(\beta_s) \cdot R_z(\gamma_s))^{\mathrm{T}} \cdot \begin{bmatrix} v_{sx} \\ v_{sy} \\ v_{sz} \end{bmatrix} \quad (1)$$

Table 5.1. Bony landmarks used for construction of the local coordinate systems

Bony landmarks	Description of palpation point
Thorax	
Processus xiphoideus, PX	Most caudal point
Incisura jugularis, IJ	Middle of notch
Proc spin 7th cerv vert, C7	Most dorsal point
Proc spin 8th thor vert, T8	Most dorsal point
Clavicle	
Sternoclavicular joint, SC	Most cranial part of joint ligament
Acromioclavicular joint, AC	Most mediocaudal point
Scapula	
Processus coracoideus, PC *	Most ventral point
Acromioclavicular joint, AC *	
Angulus Acromialis, AA *	Middle of most pronounced curvature
Trigonum spinae, TS*	End of spinal crest, in the middle
Angulus inferior, AI *	Most caudal point, middle of curvature
Humerus	
Epicondylus medialis, EM	Most caudo-dorsal point
Epicondylus lateralis, EL	Most caudo-dorsal point
Gleno-humeral joint rotation center, GH **	

**Estimated by linear regression equations from *.

where s_x, s_y, s_z, are the coordinates of position vector ${}^{G}\mathbf{S}$ being the endpoint of the stylus; o_{sx}, o_{sy}, o_{sz}, are the coordinates of the position vector $G\mathbf{O}_s$, of the stylus receiver; v_{sx}, v_{sy}, v_{sz}, are the position coordinates of the vector ${}^{R}\mathbf{V}_s$, between the stylus endpoint and the center of the stylus receiver and α_s, β_s, γ_s are the Euler angles describing the orientation of the stylus receiver.

Note that the superscript G placed in front of the vector means orientation in the global coordinate system (GCS) and the superscript R means orientation in the local coordinate system (LCS) of a Flock of Birds receiver. The vector ${}^{R}\mathbf{V}_s$ between the receiver's center and the stylus tip in the local coordinate system of the stylus receiver was established by continuous recordings of position and orientation of the stylus receiver while slowly rotating the stylus around its endpoint ${}^{G}\mathbf{S}$. Both ${}^{G}\mathbf{S}$ and ${}^{R}\mathbf{V}_s$, were then estimated by minimizing the criterion:

$$J = \sum_{i=1}^{n} e_i^2 \tag{2}$$

where

$$\begin{bmatrix} e_x \\ e_y \\ e_z \end{bmatrix} = \begin{bmatrix} s_x \\ s_y \\ s_z \end{bmatrix} - \left(\begin{bmatrix} o_{sx} \\ o_{sy} \\ o_{sz} \end{bmatrix} + (R_x(\alpha_s) \cdot R_y(\beta_s) \cdot R_z(\gamma_s))^T \cdot \begin{bmatrix} v_{sx} \\ v_{sy} \\ v_{sz} \end{bmatrix} \right) \tag{3}$$

with o_{sx}, o_{sy}, o_{sz}, α_s, β_s, γ_s, recorded by the receiver. The error was calculated at about 50 different positions in the calibrated space with about three measurements for each position. To minimize, the Levenberg-Marquardt algorithm was used. [10–12]

Using the stylus to measure the global position of the bony landmarks the vectors between the bony landmarks and the bone receivers were calculated by:

$$\begin{bmatrix} v_{bx} \\ v_{by} \\ v_{bz} \end{bmatrix} = (R_x(\alpha_b) \cdot R_y(\beta_b) \cdot R_z(\gamma_b))^T \cdot \begin{bmatrix} b_x - o_{bx} \\ b_y - o_{by} \\ b_z - o_{bz} \end{bmatrix} \tag{4}$$

where v_{bx}, v_{by}, v_{bz} are the coordinates of the vector ${}^{R}\mathbf{V}_b$ between the bone receivers and the bony landmarks; b_x, b_y, b_z, are the coordinates of position vector ${}^{G}\mathbf{B}$ of the bony landmarks; o_{bx}, o_{by}, o_{bz} are the coordinates of the position vector ${}^{G}\mathbf{O}_b$ of the bone receiver; α_b, β_b, γ_b are the Euler angles describing the orientation of the bone receiver.

In this way, the bony landmarks of the thorax (PX, IJ, C7 and T8) were related to the thorax receiver, and the bony landmarks of the humerus (EL and EM) were related to the humerus receiver. The bony landmarks of the scapula (PC, AC, AA, TS and AI) were related to the humerus receiver as well. The distance between AC and AA was calculated as a vector in a scapula LCS based on the initial measurements of AA, TS and AI.

Once the initial measurements are performed, the 3D position of the bony landmarks can be reconstructed in every position of the shoulder system from the orientation and position of the bone receivers by:

$$\begin{bmatrix} b_{bx} \\ b_{by} \\ b_{bz} \end{bmatrix} = \begin{bmatrix} o_{bx} \\ o_{by} \\ o_{bz} \end{bmatrix} + (R_x(\alpha_s) \cdot R_y(\beta_s) \cdot R_z(\gamma_s))^T \cdot \begin{bmatrix} v_{bx} \\ v_{by} \\ v_{bz} \end{bmatrix} \tag{5}$$

where b_x, b_y, b_z, are the coordinates of position vector ${}^{G}\mathbf{B}$ of the bony landmarks; o_{bx}, o_{by}, o_{bz} are the coordinates of the position vector ${}^{G}\mathbf{O}_b$ of the bone receiver; α_b, β_b, γ_b are the Euler angles describing the orientation of the bone receiver; and v_{bx}, v_{by}, v_{bz} are the coordinates of the position vector ${}^{R}\mathbf{V}_b$, between the bony landmarks and the bone receivers. As no receiver could be attached to the scapula, the procedure mentioned above could not be applied to construct the scapula LCS. Therefore, a different approach was used. After adjusting the locator over the scapula, the vectors between the endpoints of the rods and the receiver mounted on the locator were established in a similar way as used to determine the vector between the stylus receiver and the stylus endpoint. The scapula locator was slowly rotated around each rod while continuously recording the position and orientation of the receiver mounted on the locator. Equation (2) and equation (3) were then used to estimate the vectors between the locator

receiver and the rod endpoints. Using equation (5) the global positions of AA, TS and AI could then be calculated from the position and orientation of the locator receiver. AC was reconstructed in the scapula LCS from AA and vector AC-AA, calculated in the scapula LCS.

Coordinate systems

The positions of the bony landmarks were used for the definition of local coordinate systems (Table 5.2, Figure 5.2). In order to be able to construct local coordinate systems at least three non collinear bony landmarks are required. On the humerus, however, the epicondylus lateralis and medialis are the only suitable landmarks that can be discerned. The essential third one, the glenohumeral joint rotation center (GH) is es - timated from five scapula bony landmarks using linear regression equations according to Meskers et al.[13] As the regressors, namely, PC, AA, AC, TS and AI were expressed in relation to the humerus receiver, GH was estimated with respect to the humerus receiver. GH could therefore be reconstructed in every position of the shoulder from the position and orientation of the humerus receiver in the same way as the other bony landmarks were reconstructed. On the clavicle a third landmark is missing as well. A solution to this problem was proposed by Van der Helm and Pronk[5], who defined the initial z-axis of the clavicle as the vector product of the clavicular x-axis and the tho - racic y-axis.

Table 5.2. Local coordinate systems

Thorax	${}^{G}Y_t$:	$\{-({}^{G}PX+{}^{G}T8)/2\} / \|\|({}^{G}IJ+{}^{G}C7)/2-({}^{G}PX+{}^{G}T8)/2\|\|$
	${}^{G}X_t$:	perpendicular to the plane ^{G}IJ, ^{G}C7, (^{G}PX+^{G}T8)/2
	${}^{G}Z_t$:	perpendicular to ${}^{G}Y_t$ and ${}^{G}X_t$
	origin:	$({}^{G}IJ_{+}{}^{G}C7)/2$
Clavicle	${}^{G}X_c$:	$({}^{G}AC-{}^{G}SC)/\|\|{}^{G}AC-{}^{G}SC\|\|$
	${}^{G}Z_c$:	perpendicular to ${}^{G}X_c$ and ${}^{G}Y_t^{*}$, pointing backward
	${}^{G}Y_s$:	perpendicular to ${}^{G}X_c$ and ${}^{G}Z_c$
	origin:	${}^{G}SC$
Scapula	${}^{G}X_s$:	$({}^{G}AA-{}^{G}TS)/\|\|{}^{G}AA-{}^{G}SC\|\|$
	${}^{G}Z_s$:	perpendicular to $({}^{G}AI-{}^{G}AA)$ and ${}^{G}X_s$, pointing backward
	${}^{G}Y_s$:	perpendicular to ${}^{G}X_s$, and ${}^{G}Z_s$
	origin:	${}^{G}AA$
Humerus	${}^{G}Y_h$:	$\{{}^{G}GH-({}^{G}EM+{}^{G}EL)/2\}/\|\|\{{}^{G}GH-({}^{G}EM+{}^{G}EL)/2\}\|\|$
	${}^{G}Z_h$:	perpendicular to ${}^{G}Z_h$ and $({}^{G}EL+{}^{G}EM)$, pointing backward
	${}^{G}X_h$:	perpendicular to ${}^{G}Y_h$ and ${}^{G}Z_h$
	origin:	${}^{G}GH_h$

*Chosen to be aligned with the global (thorax) axis, for the lack of a third plane definition.

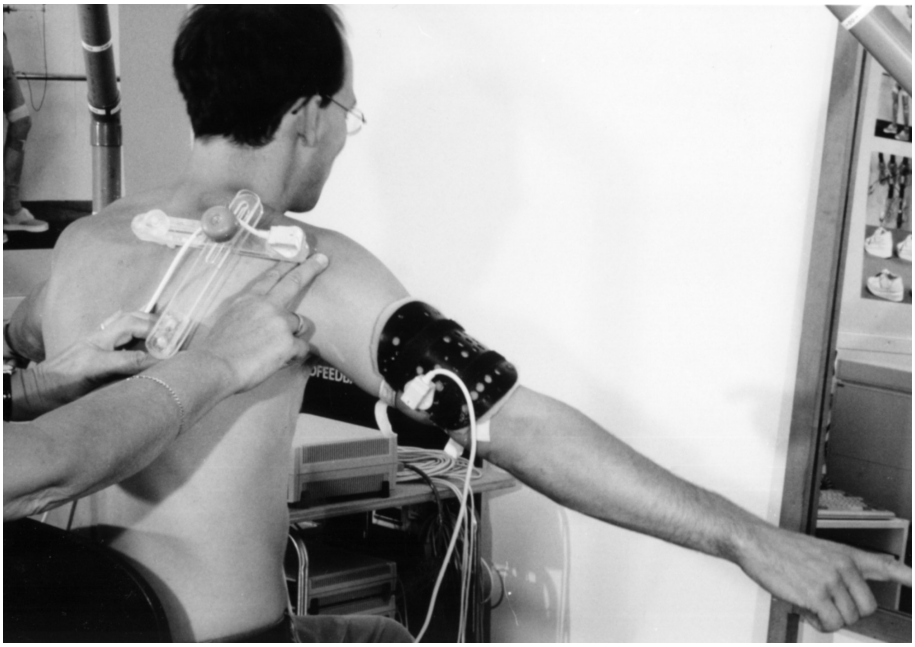

Figure 5.3. The complete measurement set-up. Two semicircular pipes besides the sitting subject function as guides while elevating the arm. Also visible is the cuff around the upper arm with a sensor attached to it.

Shoulder position measurements

After performing the initial measurements, shoulder positions were recorded during standardized humerus elevations. Two-sided humerus elevations were performed in N_E=3 elevation planes: forward flexion (90˚angle with the frontal plane), elevation in the scapular plane (30˚) and an elevation in the frontal plane (0˚). The positions were standardized by asking the subjects to point with the index finger to marks on two semi-circular pipes mounted along side the sitting subject (Figure 5.3). Recordings were started in the resting position and ended when maximal elevation was reached. The intervals between each position to be recorded were dictated by the marks on the pipes which were 10˚ apart. In each position, the scapula locator was readjusted over the scapula and the position and orientation of the receivers on the bones and the locator were subsequently recorded. The position of the scapula locator over the bony landmarks was controlled by pressing the lateral rod with the right hand on AA after palpating AA with the index finger of the same hand. The same procedure was performed for AI using the left hand and the caudal rod. TS was then reached by rotating the locator until the medial rod made contact with TS. N_s=15 subjects were measured: eight males and seven females. Mean age was 24.3 yr (SD 8.4); mean weight 67.2 kg (SD 11.1) and mean length 1.79 m (SD 0.24). Per subject, five initial measurements were performed as well as N_R=5 elevations in each plane. A complete set of initial measurements was performed before starting a new set. Each elevation was conducted in steps of 10˚,

Table 5.3 Euler decomposition orders and their physical interpretations

Bone rotations	Order	Interpretation
Thorax	*X*	Backward rotation about the axis
	Y'	Torsion about the axis
	Z"	Laterorotation about the axis
Clavicle	*Y*	Protraction about the axis
	Z'	Elevation about the *Z'* axis
	X"	Axial rotation about the *X"* axis*
Scapula	*Y*	Protraction about the *Y* axis
	Z'	Laterorotation about the *Z'* axis
	X"	Spinal tilt about the scapular spine (*X"* axis)
Humerus	*Y*	Elevation plane (axis)
	Z'	Elevation angle (*Z'* axis)
	Y"	Axial rotation about axis
Joint rotations	Order	Interpretation
AC	Y	(Protraction)** about the axis
	Z'	(Elevation)** about *Z'* axis
	X"	(Axial rotation) ** about *X"*axis
GH	Ý	Pole angle (axis)
	Z'	Humeral elevation (rotation about *Z'* axis)
	Y"	Axial rotation about axis

*Estimated; **for the AC joint, no anatomical terminology has been defined yet.

resulting in $N_p \approx 18$ positions per elevation. One full humerus elevation was regarded to be one motion, humerus elevation angles were not randomized. Between each el - evation the scapula locator was completely removed from the scapula and the subjects were allowed a short rest. The same measurements were repeated by a second observer in the same order. Per elevation plane a complete set of measurements was performed by one observer before the second observer took over the measurements. The receivers on the humerus and the thorax were not removed during the whole experiment. In order to estimate the interday variability, six subjects were measured after an average time period of 6 months.

Data processing

The bone rotations as well as the joint rotations were calculated from the orientations of the local coordinate systems. Various approaches can be used for the rotation de - scriptions: e.g., rotations with respect to the resting position or rotations with respect to the GCS. As no well-defined anatomical position for the shoulder exists, we chose to describe the rotations of the bones with respect to a virtual position in which the coordinate systems of the bones are aligned. [5,6,14] Furthermore, the orientations of the clavicle, scapula and humerus were calculated in the thorax LCS whereas the thorax

orientations were calculated in the GCS. This implies that (1) rotations start with an offset, and (2) thorax rotations are eliminated. For example, for the clavicle this is performed by calculating:

$$ {}^{T}_{C}R = {}^{G}T^{T} \bullet {}^{G}C \qquad (6) $$

where ${}^{T}_{C}R$ is the rotation from, for example, the clavicle with respect to the thorax; ${}^{G}T$ is the orientation of the thorax LCS in the GCS and ${}^{G}C$ the orientation of, for ex-

Table 5.4 Coefficients of the fifth order polynomial fits describing the average bone and joint rotations during humerus forward flexion and abduction in the frontal plant obtained from measurements on 15 subjects

	Forward flexion					
Cy	2.1853*10^{-9}	-5.5245*10^{-7}	2.4336*10^{-5}	4.1721*10^{-4}	-4.5264*10^{-2}	-1.7797*10^{1}
Cz	3.6034*10^{-9}	-1.5463*10^{-6}	2.2760*10^{-4}	-1.4124*10^{-2}	4.5182*10^{-1}	4.8646*10^{0}
Cx	-4.5909*10^{-9}	1.3651*10^{-6}	-1.3562*10^{-4}	7.9615*10^{-3}	-3.2147*10^{-2}	-4.1159*10^{-3}
Sy	-4.0875*10^{-9}	1.4623*10^{-6}	-1.9863*10^{-4}	1.1423*10^{-2}	-9.7558*10^{-2}	3.0748*10^{1}
Sz	-1.7234*10^{-9}	3.1102*10^{-7}	1.3582*10^{-5}	-3.2411*10^{-3}	3.8638*10^{-1}	8.6986*10^{-1}
Sx	5.1167*10^{9}	-1.6794*10^{-6}	1.9431*10^{-4}	-9.2401*10^{-3}	2.3396*10^{-1}	-1.2964*10^{1}
Hy	1.3304*10^{-8}	-7.1742*10^{6}	1.5034*10^{-3}	-1.5480*10^{-1}	7.7128*10^{0}	-6.8768*10^{1}
Hz	0.0000	0.0000	0.0000	0.0000	1.0000	0.0000
Hy	-1.2749*10^{-8}	6.8061*10^{-6}	-1.4212*10^{-3}	1.4420*10^{-1}	-6.9372*10^{0}	8.4357*10^{1}
ACy	-6.4917*10^{-10}	7.7762*10^{-8}	8.1834*10^{-6}	-1.2568*10^{-3}	1.5526*10^{-1}	6.2717*10^{1}
ACz	1.2187*10^{-9}	-5.8669*10^{-7}	1.0944*10^{-4}	-9.5935*10^{-3}	3.1536*10^{-1}	5.8298*10^{0}
ACx	-1.5663*10^{-9}	2.9147*10^{-7}	3.8775*10^{-6}	-2.0460*10^{-3}	1.1905*10^{-1}	-7.3438*10^{0}
GHy	-5.0757*10^{-9}	2.7554*10^{-7}	4.5126*10^{-4}	-9.4853*10^{-2}	6.2367*10^{0}	-7.7000*10^{1}
GHz	-7.4381*10^{10}	3.9648*10^{-7}	-3.0311*10^{5}	-9.0468*10^{-3}	1.8049*10^{0}	-2.6992*10^{1}
GHy	4.1409*10^{-9}	-2.5709*10^{-7}	-3.6986*10^{-4}	8.0000*10^{-2}	-5.6124*10^{0}	5.4389*10^{1}
	Abduction					
Cy	1.8567*10^{-9}	-7.4378*10^{-7}	1.2137*10^{-4}	-9.9322*10^{-3}	1.2359*10^{-1}	-1.9994*10^{1}
Cz	2.3787*10^{-9}	-8.6897*10^{-7}	1.1101*10^{4}	-7.6090*10^{-3}	4.6930*10^{-1}	1.2423*10^{0}
Cx	6.2531*10^{-10}	2.5454*10^{-7}	-3.0344*10^{-6}	7.7184*10^{-3}	-1.1281*10^{1}	3.8480*10^{-1}
Sy	1.5262*10^{-9}	-8.4824*10^{-7}	1.7366*10^{-4}	-1.4697*10^{-2}	4.0896*10^{-1}	2.5660*10^{1}
Sz	9.7808*10^{-10}	-1.5437*10^{-7}	-3.9365*10^{-5}	9.1957*10^{-3}	-7.5897*10^{-2}	3.2705*10^{0}
Sx	-1.2000*10^{-9}	4.1000*10^{-7}	-6.3591*10^{-5}	5.7831*10^{-3}	-1.1260*10^{-1}	-1.0859*10^{1}
Hy	-8.4856*10^{-9}	3.5626*10^{-6}	-5.0699*10^{-4}	3.1168*10^{-2}	-6.0840*10^{-1}	-1.6062*10^{0}
Hz	0.0000	0.0000	0.0000	0.0000	1.0000	0.0000
Hy	2.2793*10^{-8}	-8.4675*10^{-6}	1.1546*10^{-3}	-6.2878*10^{-2}	1.4284*10^{-1}	2.6782*10^{1}
ACy	-1.1813*10^{9}	3.1405*10^{-7}	-2.3510*10^{-5}	2.3346*10^{-5}	1.5125*10^{1}	6.2520*10^{1}
ACz	1.4964*10^{-9}	-5.9674*10^{-7}	8.7899*10^{-5}	-5.9951*10^{-3}	1.6775*10^{-1}	5.6662*10^{0}
ACx	-3.6751*10^{9}	1.1614*10^{6}	-1.2430*10^{-4}	6.0173*10^{-3}	-8.3862*10^{-2}	-6.8843*10^{0}
GHy	5.1421*10^{8}	-2.1094*10^{-5}	3.0906*10^{-3}	-1.8569*10^{-1}	3.8201*10^{0}	-4.0685*10^{1}
GHz	-1.1474*10^{9}	5.1756*10^{7}	-5.4938*10^{-5}	-1.7568*10^{-3}	9.8476*10^{-1}	-1.6861*10^{1}
GHy	-4.1287*10^{-8}	1.7160*10^{-5}	-2.5489*10^{-3}	1.6040*10^{-1}	-4.2576*10^{0}	2.4811*10^{1}

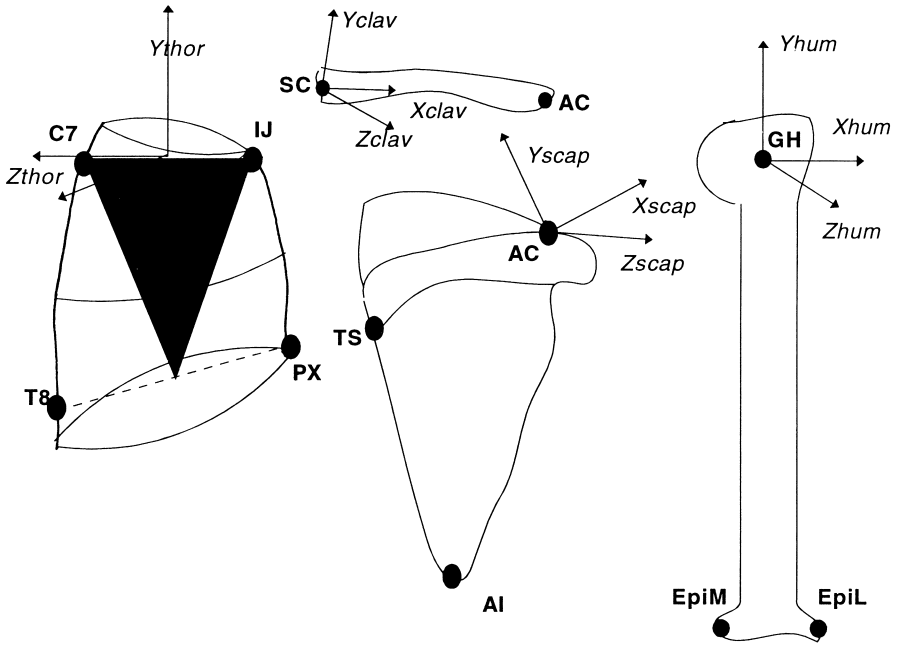

Figure 5.2. Local coordinate systems used in this study.

ample, the clavicle in the GCS. Note that the superscript T placed behind the orientation matrix means transposed.

The joint rotations are obtained by expressing the orientation of the distal bone in the LCS of the proximal bone. The rotations at, for example, the acromioclavicular joint are then calculated by:

$$ {}^{C}_{S}R = {}^{G}C^{T} \bullet {}^{G}S \qquad (7) $$

Note that the rotations at the sterno-clavicular joint are the same as the clavicle rotations, since both are calculated in thorax LCS.

The subsequent rotations about each of the three axes of the local or global coordinate systems were expressed in Cardan angles. The order of the rotations was chosen according to Van der Helm.[6] Table 5.3 gives the decomposition orders used. Note that the second and third rotations occur about rotated axes and are therefore denoted by primes and double primes. As was already noted, for the clavicle a third plane definition is absent for the lack of third bony landmark. This means the clavicle axial rotation cannot be measured directly. Van der Helm and Pronk [5] proposed a solution assuming that the axial rotations of the clavicle will mainly take place in the sternoclavicular joint. The axial rotations are then estimated by minimizing the rotations at the acromioclavicular joint.

Results

Measurement speed

After a period of training it appeared that the positioning of the scapula locator over the scapula could be performed without difficulty. Therefore, the measurement speed was gradually increased until a sample frequency of about 1 Hz could be reached. This means that one full humerus elevation, divided into about 18 measurements took ≈ 20 s. Per subject, ten initial and 30 elevation measurements were performed. As the marks on the pipes were 10° apart, each recorded elevation was represented by about 18 shoulder positions, depending on the maximal elevation the subject was able to reach and taking into account that the intervals were not always exactly 10° wide, especially near maximal elevation. This resulted in about 500 observations per subject per recording session. A complete recording session including mounting and demounting of the subject in the set-up and performing both initial and position measurements by two observers lasted about 90 min.

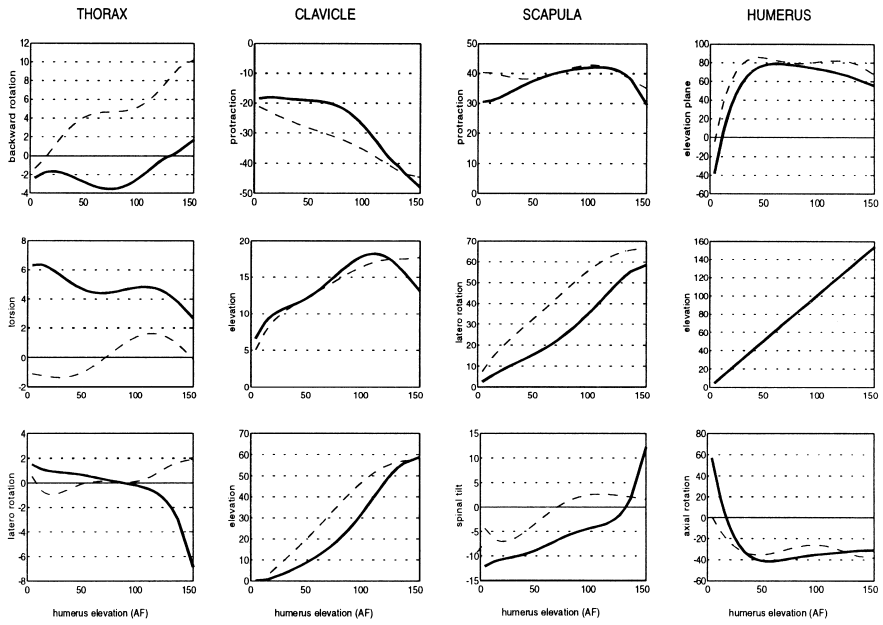

Figure 5.4. Fifth order polynomial fits to the Cardan angles describing the orientations of the bones during humerus forward flexion. The bold lines represent the orientations averaged over two observers and 15 subjects from this study. The dotted lines represent fifth order polynomial fits to orientation recordings by Van der Helm and Pronk (based on ten subjects)

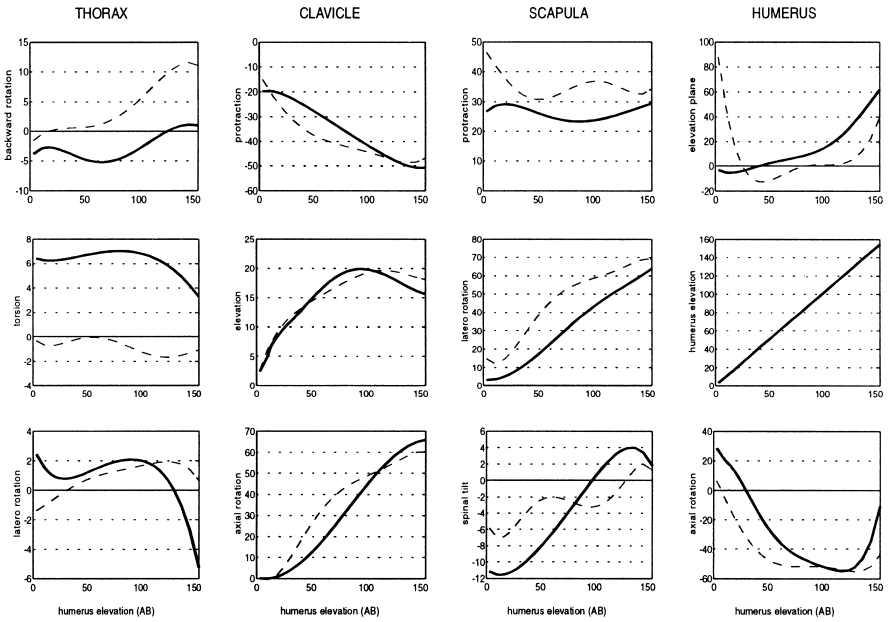

Figure 5.5. Fifth order polynomial fits to the Cardan angles describing the orientations of the shoulder bones during humerus elevation in the frontal plane (abduction). Bold lines: this study; dotted lines: Van der Helm and Pronk.

Bone rotations

An overview of the shoulder kinematics was obtained by fitting fifth order polynomials to the pooled N_R=5 repetitions of the $N_P \approx 18$ position recordings performed by the N_O=2 observers on the N_S=15 subjects. Estimations of the mean rotations of the bones and joints were thus obtained. In Figures 5.4–6 the polynomials are shown describing the bone and joint rotations during a forward flexion of the humerus and a humerus abduction in the frontal plane, respectively. The coefficients of the polynomials are listed in Table 5.4. The thorax rotations show a slight backward rotation, while the torsion and latero-rotation are minimal because the movements were performed symmetrically using both arms. The clavicle elevates and retracts during humerus elevation. The axial rotations start at zero as a result of the axial rotation estimation procedure. The clavicle rotations are fairly large, meaning that the rotations at the sternoclavicular joint are large as well. Regarding the scapula rotations, it can be seen that the scapula has a tendency to 'follow' the humerus elevation plane and it protracts more during forward flexion than it does in abduction.

The scapula latero-rotation is the only scapula rotation that is accessible by 2D viewing techniques and is therefore of importance in the literature. As can be seen, the relation between the humerus elevation and the scapula latero-rotation (scapula-hu-

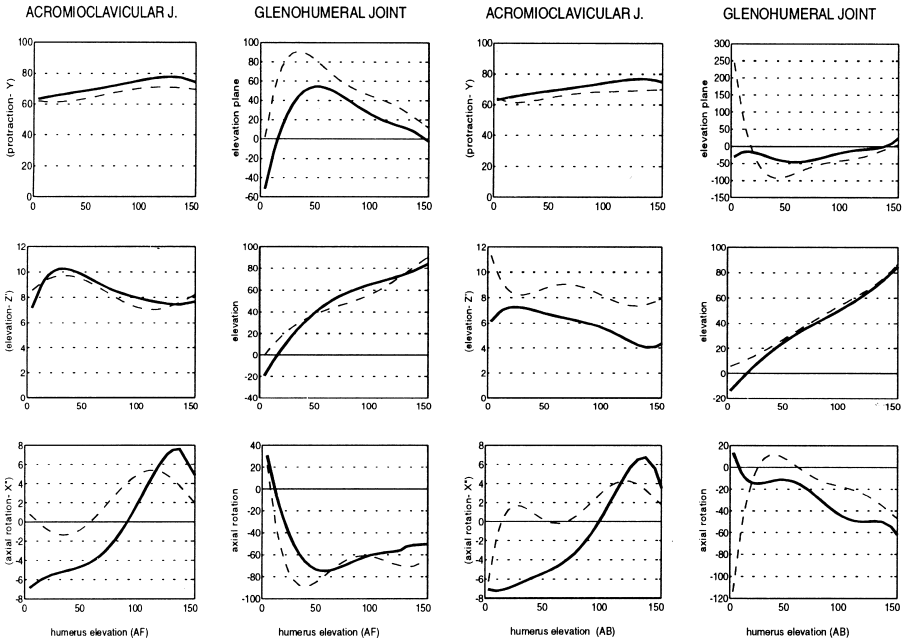

Figure 5.6. Fifth order polynomial fits to the Cardan angles describing the joint rotations during humerus forward flexion (first two columns) and abduction (last two columns), re - spectively. Bold lines: this study; dotted lines: Van der Helm and Pronk.

meral rhythm) is about 2:1. During humerus elevation, the scapula is pressed against the thorax: the spinal tilt. The humerus pole angle and axial rotation show steep slopes in the first 30° of humeral elevation, caused by interactions of the first and third rota - tions (Gimbal lock effect).

Joint rotations

Unlike the rotations at the SC joint, the rotations at the acromioclavicular joint are small as a result of the clavicle axial rotation estimation procedure. The rotations at the glenohumeral joint are the result of calculating the humerus orientations in the scapula LCS. Due to the fairly large scapula rotations during humerus elevation they differ considerably from the humerus rotations calculated with respect to the thorax. This means that the visible humerus-thorax relationship can by no means be used as a basis for studying glenohumeral relationships. The steep slopes of the glenohumeral pole angle and axial rotation during the first degrees of humerus elevation do not re - flect true rotations for they reflect Gimbal lock effects, likewise for the first and third humerus rotations with respect to the thorax.

Table 5.5. Offset, inter-trial (IT), inter- day(ID), inter- observer(IO) and inter-subject (IS) variability of bone- and joint rotations (SD, in degrees)

	AF					AB				
Rotation	Offset	IT	ID	IO	IS	Offset	IT	ID	IO	IS
Tx	0.64	1.30	3.20	1.57	5.46	0.57	1.23	3.38	1.54	5.06
Ty'	0.82	0.94	2.86	1.32	4.38	0.79	1.03	2.67	1.38	3.73
Tz"	0.72	0.68	1.80	0.82	4.04	0.71	0.70	1.75	0.90	3.24
Cy	1.98	2.38	3.33	3.40	5.93	2.68	1.90	3.10	2.61	4.57
Cz'	1.30	1.55	3.38	2.43	5.79	2.08	1.37	3.60	2.17	4.60
Cx"	0.55	3.65	4.26	5.59	7.21	0.97	3.35	3.56	5.41	5.21
Sy	1.04	2.46	4.17	3.21	9.02	1.52	2.26	4.01	2.89	7.86
Sz'	0.57	2.53	3.73	3.93	7.04	0.53	2.37	3.42	3.80	6.05
Sx"	0.73	1.96	3.03	2.73	7.81	0.73	1.93	2.83	2.87	8.02
Hy'	1.94	7.77	9.68	8.16	15.10	2.41	4.74	12.70	5.50	2.70
Hy"	5.05	7.37	10.50	7.68	20.70	5.07	4.93	10.9	5.74	19.60
ACy	2.17	1.36	2.27	2.52	4.46	2.87	1.46	2.32	2.61	4.35
ACz'	0.56	2.95	5.88	3.60	6.69	0.39	2.80	5.93	3.55	7.38
ACy"	1.20	1.81	2.47	2.59	6.99	0.59	1.61	2.29	2.89	6.34
GHy	0.66	19.6	22.20	20.70	25.50	0.81	19.40	20.3	21.10	27.00
GHz'	0.55	4.86	8.88	5.87	10.80	0.57	2.93	4.25	4.13	8.15
GHy"	5.30	19.70	22.60	0.70	26.40	5.26	19.40	21.20	21.10	30.00

Comparison with Van der Helm and Pronk

Our results were compared with results from Van der Helm and Pronk. [5] They performed position measurements on a group of ten male subjects age 23.1 yr (SD 3.1), weight 71.2 kg (SD 9.2), length 1.82 m (SD 0.21). The results from their study are plotted in Figures 4–6 as dotted lines. Their data were processed using the same protocol used in this study, however they based the scapula LCS on AC instead of AA. Furthermore, they used a different experimental procedure in the way that they measured standing subjects and restriction of head and trunk rotations.

Accuracy

The error evolving from the initial measurements was estimated by calculating the variability on one motion caused by different LCS arising from the palpation inaccuracy. Using the mean of the initial measurements, the intra-subject accuracy of the

measurements was estimated as the standard deviation of the N_R=5 repeated measurements performed on each subject, calculated per elevation plane and per observer. The standard deviation was estimated by the difference between the measured data and estimated data obtained by applying least squares fifth order polynomial fits through the $N_R * N_P \approx 90$ orientation recordings. In Table 5.5 values are presented averaged over the N_O=2 observers and the N_S= 15 subjects and shown for N_E=2 elevation. The inter-observer variance was estimated on the $N_R * N_P * N_O \approx 180$ position recordings. Table 5.5 presents values, averaged over the N_P=15 subjects and for N_E=2 elevation planes. The inter-subject variance was estimated on the $N_R * N_P * N_S \approx 1350$ orientation recordings, calculated per observer and per elevation plane. The values in Table 5.5 are averaged over the N_O=2 observers and shown for N_E=2 elevation planes. Note that all values were measured after each observer performed five repeated initial measurements per subject. Per observer, the mean of the vectors established from these initial measurements was used for further calculation.

Discussion

A full kinematic description of the shoulder girdle in 3D is obtained in this study. The measurements were static, because in each position to be recorded the arm was held still. Interpolation between the positions is made possible by the fitting of fifth order polynomials. Using planar roentgen video, De Groot [15] showed that velocity effects on the scapula-humeral rhythm were minimal, so that the static recordings can be regarded as representative for dynamic movements. Parameters that are needed for a full, dynamic analysis of the shoulder motions, namely velocity and acceleration, can of course not be obtained, however, the measured shoulder positions in this study can be used as input for a 3D shoulder model, allowing for inverse quasi-static simulations. [1,2] These kind of simulations will ignore effects of velocity and acceleration which are justifiable unless very fast, dynamic movements such as throwing are analyzed.

Regarding the kinematics obtained in this study, no large differences were found compared to the results from Van der Helm and Pronk. Especially considering the fact that a different measurement device was used, the characteristics of the subject groups differed and a different task definition was used. The fact that Van der Helm and Pronk based their scapula local coordinate system on AC instead of AA will explain much of the differences. The choice for basing the scapula local coordinate system on AA instead of AC as proposed by Van der Helm [6] is made for two reasons. First, AA is measured directly by the scapula locator whereas AC has to be reconstructed. The reconstruction of AC will mean the introduction of an additional (offset) error. Second, De Groot[14] showed that basing the scapula coordinate system on AA will reduce noise introduction to the scapula angles due to Gimbal lock effects near maximal arm elevation.

In order to gain a full kinematic description, assumptions are made concerning the fixed position of the glenohumeral joint in the scapula local coordinate system and the axial rotation of the clavicle, which can each be justified well. The axial rotation of the clavicle in the acromioclavicular joint will be restricted by the strong trapezoid and

conoid ligaments.[5] This effect was actually found when simulating shoulder kinematics using a 3D shoulder model.[1] GH has a fixed position with respect to the scapula if GH behaves like a perfect ball and socket joint. That this is indeed the fact can be argued from the joint geometry which shows equal radii of glenoid and humeral head in a number of studies[13,16–18] and from the fact that it is mechanically disadvantageous to have joint with 'play'.[19]

It can therefore safely be assumed that a fairly precise description of shoulder kinematics is obtained. Further refinement can be obtained by estimating a more precise localization of the acromioclavicular and sternoclavicular joint rotation centers.

Van der Helm[6] proposed a standard protocol for measuring and describing shoulder kinematics. Using protocols will facilitate data comparisons and data exchange between research groups. The coordinate systems and rotation sequence in the proposal by Van der Helm[6] are chosen in such a way that global and local coordinate systems are as much as possible initially aligned, that the rotations around the axes do not deviate too much from what is commonly used in medical literature and that Gimbal lock effects are minimal. The choice for describing the rotations of the clavicle, scapula and humerus with respect to a virtual reference position means that an absolute orientation of the bones is obtained. Pronk[4] and Johnson[9] described the scapula rotations relatively with respect to a resting position. In this way, variability due to scapula position offset is eliminated but information about the global movement is lost.

After learning to position the scapula locator over the scapula in the most easy way, it appeared to be possible to reach a recording speed of about one arm position per second. This resulted in the recording of about 500 arm positions per session. In the total study, the shoulder kinematics during about 7500 arm positions were obtained. It can easily be seen that this opens wide possibilities for performing measurements on large groups of patients. The latter will be much harder when using, for example, invasive methods as Hoffman pins or tantalum balls. [20,21] Though these methods will undoubtly have a higher intrinsic measurement accuracy, this advantage will be overruled by the relative inability of gaining large quantities of data. An additional problem when using invasive methods is that they are not allowed in most countries by ethical committees. Furthermore, it is unknown to what extent invasive methods will affect the shoulder kinematics whereas it is of importance to measure the shoulder kinematics with as little restriction as possible.

There is, however, another restriction to the use of invasive markers. When, for example, tantalum balls are implanted in the shoulder bones, their positions should be recorded with respect to bony landmarks on the thorax and humerus, otherwise no geometry-based local coordinate systems can be constructed and no standardized, comparable results are obtained. The need for linkage to bony landmarks will mean that the originally high measurement accuracy will be diminished. It is not unlikely that in such a case the accuracy of the measurements will then become comparable to the accuracy found for the methodology described in this paper. No linkage to shoulder geometry of either markers, sensors or pins will result in a relatively low intra-subject variance, because this noise will be determined by the accuracy of the measurement system. On the other hand, the inter-subject but even more important the inter-day variability will be relatively high, for exact replacement of sensors or pins is not pos-

sible. This explains the relatively low intra-subject variability found by Johnson et al. [9] compared to results found by De Groot[14] and this study. Johnson et al found the intra-subject variability of the scapula rotations to be even below 2° where De Groot found intra-subject variability of 5.4, 3.7 and 4.4° for scapula protraction, laterorotation and spinal tilt, respectively, which are comparable to our results. In the results of Johnson, the error caused by bony landmark linkage of the coordinate systems was absent for they only made use of a scapula local coordinate system. The magnitude of the different errors is given in Table 5.5. It can be seen that the error caused by palpation of thorax and humerus bony landmarks causes a certain (offset) error. This error should be added to the intra-trial variability in order to get the real intra-subject error. It can then be seen that the intra-subject error becomes about as high as the inter-day and inter-observer variance, where the palpation error is already incorporated. No linkage to bony landmarks therefore means that the intra-subject variability will be very low compared to the inter-day, inter- observer and inter-subject variability, because the influence of sensor placement on the variability is eliminated. Using initial measurements as performed in this study eliminates the influence of sensor placement. The accuracy is then entirely determined by the ability to locate bony landmarks. As is shown by the low offset errors caused by the palpation and the fact that the inter-day variability is not high, it can be seen that the bony landmark retrieval is not difficult. Even after 6 months, for each subject characteristic geometric features, bony landmarks can be retrieved quite easily.

Furthermore, there is another not unimportant source of noise that cannot be eliminated using highly accurate measurement techniques which is the noise caused by the fact that a subject's movements are never exactly the same. This so-called motor noise was estimated by Groot[14] to be up to 48% of the total intra-subject variability.

In conclusion it can be stated that a useful methodology for measuring 3D shoulder positions in a clinical setting is obtained. The measurements are fast and easy to perform. Local coordinate systems are constructed on bony landmarks, which means that standardized bone positions are obtained which reduces the inter-day, inter-observer and inter-subject variability. Using other methods with high measurement accuracy, e.g., invasive techniques, will most likely not lead to a higher accuracy compared to this method due to the need of geometrical linkage of coordinate systems and the occurrence of motor noise. A disadvantage of the method is that only static or quasi-static measurements can be performed unlike invasive techniques.

Further research will focus on left-right differences and day-to-day variability of shoulder kinematics. The identification of parameters that influence the scapulohumeral rhythm by multiple regression analysis may be of help to deal with the inter-subject variability, thus enhancing the discriminative value.

Acknowledgements

The help of Mr Hans Fraterman in constructing the hardware is greatly acknowledged.

References

1. Van der Helm FCT. Analysis of the kinematic and dynamic behavior of the shoulder mechanism. *J Biomech.* 1994;27:527–550.
2. Van der Helm FCT. A finite musculoskeletal model of the shoulder mechanism. *J Biomech.* 1994;27:55l–569.
3. De Leest o, Van der Helm FCT, Rozendaal LA, Rozing PM. The influence of gleno - humeral prosthesis geometry and placement on shoulder muscle forces. *Clin Orthop.* 1996;330:222–233.
4. Pronk GM. Three-dimensional determination of the position of the shoulder girdle dur - ing humerus elevation. In: De Groot G, Hollander AP, Huijing PA, Van lngen Schenau GJ, editors *Proc 11th ISB-Congr. Biomechanics XI-B* . Amsterdam: Free University Press, 1987: 1070–76.
5. Van der Helm FCT, Pronk GM. Three dimensional recording and description of mo - tions of the shoulder mechanism. *J Biomech Eng.* 1995;177:27–40.
6. Van der Helm FCT. A standardized protocol for motion recordings of the shoulder. In: Veeger HEJ, Van der Helm FCT, Rozing PM, editors *Proc 1st Conf Int Shoulder Group* . Delft. 1997: 27–28.
7. Paul JP, Morris JRW. CAMARC II - data exchange. What? Why'? How? In: *Proc. Workshop 'CAMARC II: problems and perspectives'.* Rome, 1992.
8. Pronk GM, Van der Helm FCT. The palpator, an instrument for measuring the three dimensional positions of bony landmarks in a fast and easy way. *J Med Eng Techn* 1989;15:15–20.
9. Johnson GR, Stuart PR, Mitchell S. A method for the measurement of three dimen - sional scapular movement. *Clin Biomech* 1993;8:269–273.
10. Levenberg K. A method for the solution of certain non linear problems in least squares. *Quart Appl Math* 1944;2:164–168.
11. Marquardt DW. An algorithm for least squares estimation of non linear parameters. *J Appl Math* 1963;11:431–441.
12. Ljung L. *System identification: theory for the user* . Englewood Cliffs, NJ: Prentice-Hall, 1987.
13. Meskers CGM, Van der Helm FCT, Rozendaal LA, Rozing PM. In vivo estimation of the glenohumeral joint rotation center from scapula bony landmarks by linear regres - sion. *J Biomech*, 1998;31:93–96.
14. De Groot JH. The variability of shoulder motions measured by means of palpation. *Clin Biomech*, in press.
15. De Groot JH, Valstar ER, Arwert HJ. Velocity effects on the scapulohumeral rhythm. *Clin Biomech*, in press.
16. Meskers CGM, Van der Helm FCT, Rozendaal, LA, Rozing PM. On the use of the rotation center of the glenohumeral joint for the local coordinate system of the humerus for in vivo motion recording studies. In: Veeger HEJ, Van der Helm FCT, Rozing PM. Proc 1th Conf Int Shoulder Group. Delft, 1997: 27–28.
17. Soslowski LJ, Flatow EL, Bigliani LU,. Mow VC. Articular geometry of the glenohu - meral joint. *Clin Orthop* 1992:285:181–190.
18. Van der Helm FCT. Geometry parameters for musculoskeletal modelling of the shoul -

der system. *J Biomech* 1992; 25: 129–144.

19. Rozendaal LA. *Shoulder stability: intrinsic muscle properties and reflexive control* . PhD thesis, Delft University of Technology, The Netherlands, 1997.
20. Harryman DT, Sidles JA, Clark JM, McQuade KJ, Gibb TC, Matsen FA. Translation of the humeral head on the glenoid with passive glenohumeral motion. *J Bone Joint Surg* 1990;72A:1334–1343.
21. Högfors C, Peterson B, Sigholm G, Herberts PJ. Biomechanical model of the human shoulder joint - II. The shoulder rhythm. *J Biomech* 1991;24:699–709.